

# DGAE: Diffusion-Guided Autoencoder for Efficient Latent Representation Learning

Dongxu Liu

Institute of Automation, Chinese  
Academy of Sciences  
Beijing, China

Jiahui Zhu

Independent Researcher  
China

Yuang Peng

Tsinghua University  
Beijing, China

Haomiao Tang

Tsinghua University  
Beijing, China

Yuwei Chen

Institute of Computing Technology,  
Chinese Academy of Sciences  
Beijing, China

Chunrui Han

StepFun  
Beijing, China

Zheng Ge

StepFun  
Beijing, China

Daxin Jiang

StepFun  
Beijing, China

Mingxue Liao\*

Institute of Automation, Chinese  
Academy of Sciences  
Beijing, China

## Abstract

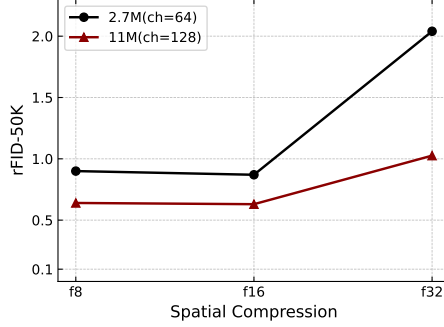
Autoencoders empower state-of-the-art image and video generative models by compressing pixels into a latent space through visual tokenization. Although recent advances have alleviated the performance degradation of autoencoders under high compression ratios, addressing the training instability caused by GAN remains an open challenge. While improving spatial compression, we also aim to minimize the latent space dimensionality, enabling more efficient and compact representations. To tackle these challenges, we focus on improving the decoder’s expressiveness. Concretely, we propose DGAE, which employs a diffusion model to guide the decoder in recovering informative signals that are not fully decoded from the latent representation. With this design, DGAE effectively mitigates the performance degradation under high spatial compression rates. At the same time, DGAE achieves state-of-the-art performance with a 2x smaller latent space. When integrated with Diffusion Models, DGAE demonstrates competitive performance on image generation for ImageNet-1K and shows that this compact latent representation facilitates faster convergence of the diffusion model.

## Keywords

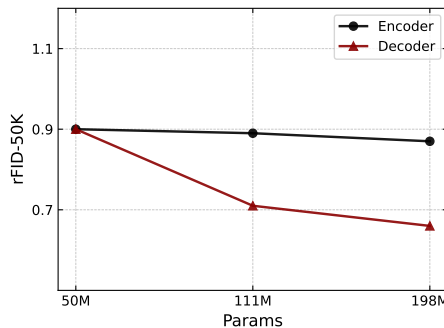
Autoencoder, VAE, Diffusion Model, GAN

## 1 Introduction

Autoencoders serve as a foundational component in modern high-resolution visual generation. Their ability to compress vast, high-dimensional image data into a compact and information-rich latent space is crucial for the efficiency and success of subsequent generative processes, most notably demonstrated by Latent Diffusion Models (LDMs) [2, 6, 7, 53, 63]. By operating within this lower-dimensional latent space, powerful models like diffusion can be trained and perform inference far more efficiently. The success of latent-based generative frameworks relies not only on powerful generative models but also significantly on the quality of the autoencoder, which constructs the latent space where generation occurs. A



(a) Scale up the discriminator.



(b) Scale up the encoder and decoder.

**Figure 1:** (a) Scaling up the discriminator in GANs can mitigate the decline in reconstruction accuracy of autoencoders under high spatial compression rates, while also enhancing reconstruction performance at low spatial compression rates. (b) Scaling up the decoder effectively improves the reconstruction quality of the autoencoder, while scaling up the encoder has little effect.

\*Corresponding Authors.

fundamental challenge lies in the inherent trade-off between spatial compression and reconstruction fidelity, as aggressive compression lowers computational cost but compromises the visual quality of autoencoder reconstructions [63].

The trade-off between compression and reconstruction fidelity remains a non-trivial problem to resolve. DCAE [10] addresses this challenge by incorporating residual connections during both down-sampling and up-sampling stages, thereby achieving higher spatial compression rates without degrading reconstruction quality. In this work, we investigate a complementary direction that focuses on the training objectives. As shown in fig. 1(a), we observe that the commonly used GAN loss [43] not only enhances the perceptual quality of reconstructed images, but that increasing the discriminator capacity further mitigates the degradation typically caused by aggressive compression. We hypothesize that **a stronger discriminator provides richer learning signals, thus enhancing the expressiveness of the decoder**.

To validate this hypothesis, we independently scaled the parameter sizes of both the encoder and decoder. Interestingly, we found that **increasing decoder capacity yields substantial improvements in reconstruction quality, while enlarging the encoder has minimal impact**, as shown in fig. 1(b). This result suggests that the decoder plays a dominant role in maintaining visual fidelity under high compression, indicating that future optimization efforts should prioritize decoder design.

Although GAN-guided VAEs have addressed the challenge of high spatial compression, they suffer from issues such as **mode collapse** and **sensitivity to hyperparameters**, making them less ideal for guiding the decoder to learn robust latent representations. In recent years, diffusion models have emerged as a dominant paradigm in visual generation due to their stable training dynamics and theoretically grounded framework. However, their potential in representation learning remains underexplored.

In this work, we propose DGAE, a novel and stable autoencoder architecture that leverages a diffusion model [30, 33] to guide the decoder in learning a denser and more expressive latent space. As illustrated in fig. 2, unlike GAN-guided methods such as SD-VAE [63], our approach conditions on the encoder’s latent representation and reconstructs the image by progressively denoising from random noise. The core idea is to **transfer the strong data modeling capabilities of diffusion models into the decoder of autoencoder**, thereby enhancing its ability to reconstruct high-frequency visual signals such as text and textures.

We demonstrate that DGAE addresses the reconstruction quality degradation and training instability observed in GAN-guided VAEs under high spatial compression, while also accelerating diffusion model training. Notably, DGAE achieves comparable reconstruction performance to SD-VAE with a significantly smaller latent size. Furthermore, we show that optimizing for high spatial compression is not the sole objective in autoencoder design—**smaller latent representations can also facilitate faster convergence in downstream generative models (section 4.4)**.

In summary, our contributions are as follows:

- We analyze conventional autoencoder designs and empirically show that the decoder plays a critical role in determining reconstruction quality.

- We introduce DGAE, a diffusion-guided autoencoder that achieves more compact and expressive latent representations.
- We demonstrate that smaller latent representations not only enable high compression but also accelerate training in diffusion-based generative models.

## 2 Preliminaries

To facilitate comprehension of our work, we provide a concise overview of the continuous visual tokenization and diffusion model.

### 2.1 VAEs

Variational Autoencoders (VAEs) [40] introduce a **probabilistic framework** for learning latent representations by **modeling the underlying data distribution**. Given an image  $\mathbf{X} \in \mathbb{R}^{H \times W \times 3}$ , the encoder  $q_\phi$  maps it to a latent representation  $\mathbf{z} \in \mathbb{R}^{\frac{H}{f} \times \frac{W}{f} \times c}$  using a downsampling factor  $f$ , and the decoder  $p_\theta$  reconstructs the image  $\hat{\mathbf{X}}$  from  $\mathbf{z}$ .

**The core objective of a VAE is to maximize the Evidence Lower Bound (ELBO)**, which consists of two terms: (1) a **likelihood term** that encourages the decoder to assign high probability to the observed data given the latent variable, and (2) a **KL divergence term** that regularizes the latent distribution to match a prior, typically a standard Gaussian. The ELBO is defined as:

$$L(\theta, \phi) = \mathbb{E}_{q_\phi(z|x)} [\log p_\theta(x|z)] - \text{KL}(q_\phi(z|x) \| p(z)) \quad (1)$$

where  $q_\phi(z|x)$  is the variational posterior approximated by the encoder, and  $p_\theta(x|z)$  is the generative likelihood modeled by the decoder. The first term, also referred to as the **reconstruction term**, depends on the assumed form of  $p_\theta(x|z)$ —for example, **under the common assumption that  $p_\theta(x|z)$  is a Gaussian distribution with fixed unit variance**, this term becomes equivalent to a mean squared error ( $\ell_2$ ) loss. Consequently, the overall VAE training objective comprises the reconstruction loss  $\mathcal{L}_{\text{REC}}(\mathbf{X}, \hat{\mathbf{X}})$  and the KL divergence loss  $\mathcal{L}_{\text{KL}}$ .

To enhance the visual quality of reconstructions, recent VAE variants have incorporated additional supervision. One such term is the perceptual loss  $\mathcal{L}_{\text{LPIPS}}$ , which utilizes feature maps extracted from a pretrained VGG network [35] to **improve perceptual similarity**. Another is the adversarial loss  $\mathcal{L}_{\text{GAN}}$ , which **refines texture details through PatchGAN-style training** [34]. The full loss function of the autoencoder can be written as:

$$\mathcal{L}_{\text{VAE}} = \alpha \mathcal{L}_{\text{REC}} + \beta \mathcal{L}_{\text{KL}} + \eta \mathcal{L}_{\text{LPIPS}} + \lambda \mathcal{L}_{\text{GAN}} \quad (2)$$

where  $\alpha, \beta, \eta, \lambda$  are weighting coefficients that balance the contribution of each term.

### 2.2 Diffusion Models

Diffusion models [30, 70] are a class of likelihood-based generative models that synthesize data by learning to reverse a progressive noising process. Similar to VAEs, diffusion models aim to maximize the data likelihood, but they do so by **modeling the data distribution through a parameterized denoising process** rather than explicit latent variational inference.

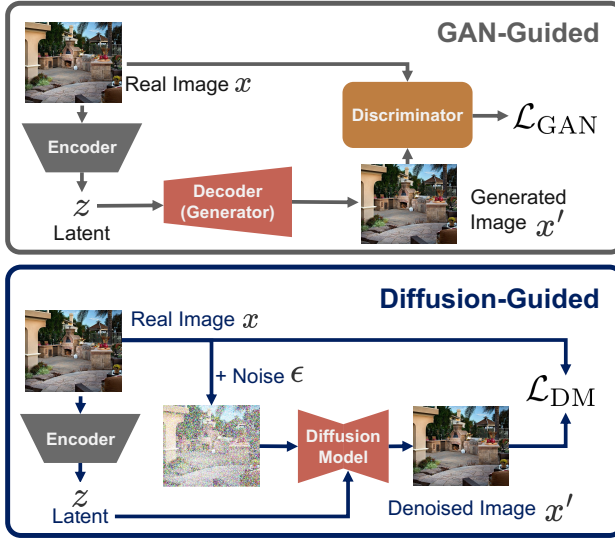


**Figure 2: DGAE is a diffusion-guided autoencoder, which is dedicated to enhancing the decoding capability of the decoder. Compared with GAN-guided methods, the latent representation  $z$  is no longer used for direct image reconstruction. Instead, it serves as a supervisory signal for the decoder, thereby better constraining  $p(x|z)$  to the data distribution  $p(x)$ .**

From a score-based perspective, these models learn to approximate the score function  $\nabla_x \log p_t(x)$ —i.e., the gradient of the log-density of the data corrupted by noise at time  $t$ . The forward process incrementally perturbs a clean image  $x_0$  into a noisy version  $x_T$  through a Markov chain, often using Gaussian noise. The reverse process then reconstructs the data by learning a sequence of denoising steps that recover  $x_0$  from  $x_T$ .

Formally, given a perturbation kernel  $q(x_t|x_0)$  that defines the forward process, the score-based model is trained to match the true score  $\nabla_{x_t} \log q(x_t|x_0)$  using a parameterized neural network  $s_\theta(x_t, t)$ . This training objective is typically framed as a denoising score matching loss [33, 46, 69, 70, 79]:

$$\mathcal{L}_{\text{DSM}} = \mathbb{E}_{x_0, t, x_t} \left[ |s_\theta(x_t, t) - \nabla_{x_t} \log q(x_t|x_0)|^2 \right]. \quad (3)$$

After training, data samples can be generated by solving a stochastic differential equation (SDE) or its discretized form using the learned score function. Compared to GANs, diffusion models offer **more stable training** and **better likelihood estimates**, making them an attractive alternative for generative modeling and image reconstruction tasks.

### 3 Approach

Our primary innovation demonstrates that visual reconstruction is inherently a generative task, and the supervision of stronger generative models can significantly boost the decoder decoding capabilities. Figure 2 illustrates the training process of DGAE.

### 3.1 From Gaussian to Diffusion Decoder

In a standard VAE, the reconstruction term of the ELBO is defined as the expected log-likelihood of the observed data under the decoder distribution  $p_\theta(x|z)$ . The first term in eq. (1) measures how well the decoder can reconstruct the original input  $x$  from the latent variable  $z$  sampled from the encoder. In practice, this expectation is estimated by Monte Carlo sampling with  $J$  samples, leading to

$$\mathbb{E}_{q_\phi(z|x)} [\log p_\theta(x|z)] \approx \frac{1}{J} \sum_{j=1}^J \log p_\theta(x|z_j), \text{ where } z_j \sim q_\phi(z|x). \quad (4)$$

To make this objective tractable, conventional VAE methods typically assume the decoder distribution  $p_\theta(x|z)$  to be an isotropic Gaussian with fixed variance, i.e.,

$$p_\theta(x|z) = \mathcal{N}(x; \mu_\theta(z), \sigma^2 I). \quad (5)$$

Under this assumption, maximizing  $\log p_\theta(x|z)$  becomes equivalent to minimizing an  $\ell_2$  reconstruction loss between  $x$  and  $\hat{x} = \mu_\theta(z)$ :

$$\mathcal{L}_{\text{REC}} = \|x - \hat{x}\|_2^2. \quad (6)$$

However, this **Gaussian assumption imposes limitations on the expressiveness of the decoder**, especially for modeling complex, high-frequency structures such as textures and detailed semantics.

To overcome this limitation, we **replace the Gaussian decoder with a conditional diffusion model**, thereby removing the restrictive Gaussian assumption and allowing the model to directly learn the score function  $\nabla_x \log p(x|z)$ . Consequently, we reinterpret this expectation as being indirectly maximized via the following score-based surrogate objective:

$$\mathcal{L}_{\text{DSM}} = \mathbb{E}_{q(x_t|x)} \left[ \lambda(t) \|s_\theta(x_t, t, z) - \nabla_{x_t} \log q(x_t|x)\|^2 \right] \quad (7)$$

which serves as a proxy for maximizing  $\log p_\theta(x|z)$  without assuming a tractable likelihood form.

In this setup, the **decoder becomes a denoising network trained to reverse a fixed forward noising process conditioned on the latent variable  $z$** . That is, given a clean image  $x$  and its corresponding latent representation  $z$ , we perturb  $x$  into a noisy sample  $x_t$  using a diffusion process  $q(x_t|x)$ , and then train a conditional score network  $s_\theta(x_t, t, z)$  to predict the gradient of the log-likelihood at each noise level as shown in fig. 2.

### 3.2 Training Objectives

The above formulation replaces the original  $\ell_2$  reconstruction loss with a denoising score matching loss, which can be interpreted as a **likelihood-based training objective under the score-based generative modeling framework**. Consequently, our model benefits from a more expressive and theoretically grounded decoder, significantly improving its ability to reconstruct fine-grained structures while maintaining the probabilistic rigor of the ELBO formulation.

In addition to the score-based loss, we find that incorporating the **perceptual loss further enhances the perceptual quality of reconstructed images**. However, since our reconstruction is now guided by a diffusion process, we must adapt the perceptual loss to align with our score-based training procedure. Specifically, during training, the model performs single-step predictions of the clean

image via  $x'_0 = x_t - t \cdot v_\theta(x_t, t, z)$ , where  $v_\theta$  is the predicted noise (or velocity). To make perceptual loss compatible with this formulation, we compute it between the predicted  $x'_0$  and the ground-truth image  $x$ , effectively supervising the model with perceptual feedback at each timestep.

Therefore, our final training objective combines the denoising score matching loss and the perceptual loss, and is defined as follows:

$$\mathcal{L}_{\text{DGAE}} = \alpha \mathcal{L}_{\text{DSM}} + \beta \mathcal{L}_{\text{KL}} + \eta \mathcal{L}_{\text{LPIPS}} \quad (8)$$

### 3.3 Architecture

**Encoder.** Similar to SD-VAE, DGAE employs a convolutional network architecture to map the input image  $x$  to the latent representation  $z$ . The distribution of  $z$  is as follows:

$$q_\phi(z|x) = \mathcal{N}(z; \mu_\phi(x), \sigma_\phi(x)^2) \quad (9)$$

where  $\sigma_\phi(x)$ ,  $\mu_\phi(x)$  are obtained by splitting the encoder’s output  $f_\phi(x)$ . Then,  $z$  is sampled from  $q_\phi(z|x)$  through reparameterization.

**Decoder.** Unlike previous deterministic decoding, the decoding task in DGAE begins with a random noise. Specifically, the diffusion process utilizes latent representations  $z$  as conditional information, gradually denoising random noise  $x_T$  to the original image  $\hat{x}$ :

$$p_\theta(\hat{x}|z) = p(x_T) \prod_{t=1}^T p_\theta(\hat{x}_{t-1}|\hat{x}_t, z) \quad (10)$$

where  $\hat{x}_t$  represents the reconstructed image at time step  $t$ . The latent representation  $z$  constrains the generation results of the diffusion process to the data distribution of the input image, while the iterative denoising of the diffusion process enhances the autoencoder’s ability to model high-frequency details and local structures.

## 4 Experiments

To validate the effectiveness of DGAE, we begin by outlining the experimental setup (section 4.1). We then assess the reconstruction performance of DGAE (section 4.2) and examine the effectiveness of its learned latent space for diffusion models (section 4.3). Finally, we analyze why DGAE outperforms SD-VAE in section 4.4.

### 4.1 Setup

**Implementation Details.** The encoder architecture of DGAE remains consistent with that of SD-VAE, while the decoder follows the standard convolutional U-Net architecture of ADM. We implemented three different latent sizes: 4096, 2048, and 1024, with each size corresponding to a distinct spatial compression ratio. For conditional denoising in the decoder, we first upsample the latent representation to pixel level using nearest-neighbor interpolation, and then concatenate it with random noise along the channel dimension.

**Data.** All reconstruction and generation experiments are conducted on the ImageNet-1K dataset [17] to evaluate the performance of DGAE. We preprocess all images by resizing them to a resolution of  $256 \times 256$  pixels. During training, we apply standard data augmentation techniques, including random cropping and random horizontal flipping, to encourage robustness and improve generalization. For evaluation, center cropping is used to ensure stable and consistent results.

**Baseline.** To assess the effectiveness of our approach, we compare it with SD-VAE [63], a widely adopted baseline in visual generation. Compared to the single-step decoding of SD-VAE, DGAE conditions on the latent representation and performs multi-step denoising of Gaussian noise to recover the original image. Aside from architectural differences, both models are trained under identical settings to ensure a fair and controlled comparison.

**Training.** We train all models with a batch size of 96, matching the configuration used in SD-VAE. All model parameters are randomly initialized and optimized using AdamW ( $\beta_1 = 0.9$ ,  $\beta_2 = 0.95$ ,  $\epsilon = 1e-8$ ) with an initial learning rate of  $1e-4$ , linearly warmed up for the first 10K steps and decayed to  $1e-5$  using a cosine scheduler. We apply a weight decay of 0.1 for regularization and clip gradients by a global norm of 1.0. To accelerate training, we adopt mixed-precision training with bfloat16.

**Evaluation.** We employ a range of metrics to comprehensively evaluate both reconstruction and generation performance. For reconstruction, we report PSNR and SSIM [32] to assess pixel-wise accuracy and perceptual similarity, respectively. Additionally, we adopt the Fréchet Inception Distance (rFID) [27], computed between the original and reconstructed images, as a more perceptually aligned metric. Notably, we use the rFID, calculated on a fixed subset of 5K images from the ImageNet-1K [17] validation set. For generation, we evaluate the synthesized samples using several standard metrics [18]: generation FID (gFID), sFID [50], Precision, and Recall. These metrics collectively measure fidelity, diversity, and sample quality of the generated outputs, providing a thorough assessment of the generative capabilities of our model.

### 4.2 The reconstruction capability of DGAE

We first demonstrate that DGAE achieves better reconstruction results with higher spatial compression rates and smaller latent sizes, proving its ability to learn more expressive latent representations. Then, as discovered in SD-VAE, scaling up the decoder can effectively enhance the reconstruction performance of DGAE. Unless otherwise specified, DGAE-B is used by default in the experiments of this section.

**Spatial Compression.** To verify whether the Diffusion Model can mitigate the performance degradation under high spatial compression rates like GAN, we test DGAE in latent spaces with various spatial compression rates. As shown in table 2, DGAE achieves superior performance across all spatial compression rates. Qualitatively, as shown in fig. 3, we find that DGAE is capable of modeling better texture features and symbols. The results further confirm that the encoder has already stored the semantics of the image in the latent representation, and what we need to do is to uncover it.

**Latent Compression.** Moreover, under higher spatial compression rates, increasing the number of latent channels can improve the reconstruction performance of autoencoders. However, this comes at the cost of significantly larger diffusion models and more challenging optimization [87]. This motivates the use of a more compact latent space. We investigate the ability of DGAE to mine information by fixing the spatial compression rate and reducing the number of channels in the latent representation. As shown table 2, the gap between DGAE and SD-VAE widens as the latent size

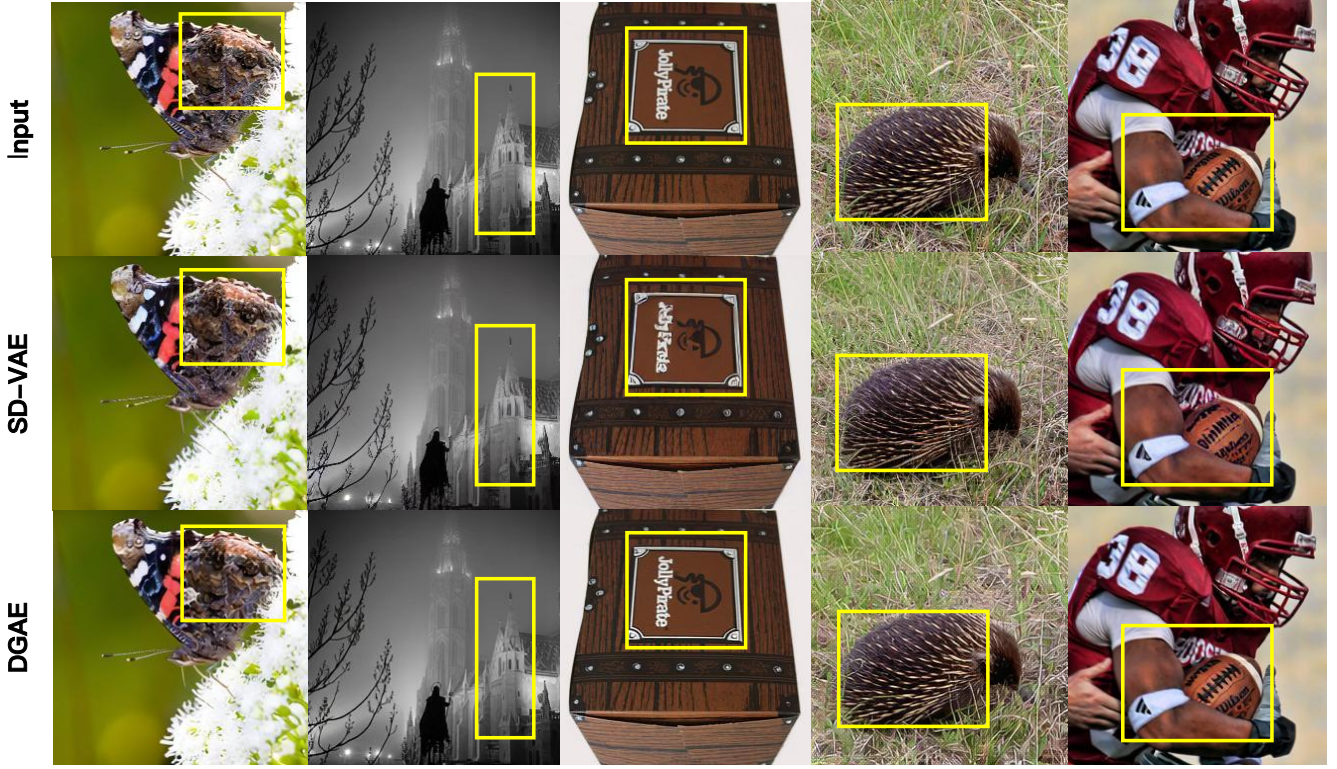


Figure 3: Reconstructed samples of DGAE and SD-VAE. These results suggest that, despite employing a simpler combination of losses, DGAE benefits from the strong modeling capacity of the diffusion decoder, leading to more effective recovery of fine-grained details such as textures and structural patterns.

Table 1: Reconstruction Results of Scaled-Up DGAE on ImageNet 256 × 256. A larger decoder architecture (Unet) in DGAE leads to improved quantitative reconstruction results.

Autoencoder	Total Params	Decoder Arch			Reconstruction Performance		
		Unet <sub>channel</sub>	$t_{emb}$	Params	rFID-5k↓	PSNR↑	SSIM↑
DGAE-B	157M	128	512	122M	4.23	25.73	0.76
DGAE-M	310M	192	768	276M	3.76	26.10	0.76
DGAE-L	525M	256	1024	491M	3.58	26.13	0.77

decreases. In addition to the quantitative results, fig. 4 shows image reconstruction samples produced by SD-VAE and DC-AE. The reconstructed images by DGAE demonstrate better visual quality than those reconstructed by SD-VAE. In particular, for autoencoders with a latent size of 1024, DGAE still maintains good visual quality for small text and human faces.

**Scalability.** As emphasized in section 1, the decoder plays a central role in autoencoder architectures. To evaluate the scalability of DGAE, we fix the encoder and progressively scale the decoder. Specifically, we construct three variants with increasing model capacities: DGAE-B, DGAE-M, and DGAE-L. The number of parameters and detailed configurations of the corresponding U-Net decoders are provided in table 1. As shown in fig. 5, larger decoders significantly enhance the model’s ability to capture structural and fine-grained image details. Quantitative results in table 1 further support this observation, demonstrating that DGAE is a scalable and effective autoencoder framework.

While good latent representations should enable faithful reconstruction from the pixel space, its true utility lies in how effectively it supports downstream generative modeling. In particular, a meaningful and compact latent space should facilitate the training of powerful diffusion models. Therefore, in section 4.3, we evaluate whether the representations learned by DGAE contribute to improved image synthesis performance.

### 4.3 Latent Diffusion Model

We compare the performance of training a latent diffusion image generation model on two different latent representations, learned by DGAE or SD-VAE. Specifically, we use DiT-XL1 [53] as the latent diffusion model for class-conditional image generation on ImageNet-1K[17]. In this section, our focus is to demonstrate the effectiveness of the latent representation learned by DGAE. Therefore, we train the diffusion model for only 1M steps instead of the original 7M steps [53].



Figure 4: Reconstruction samples with different latent sizes. The result was obtained under a fixed spatial compression rate of f16, with the channel dimension of the latent representation gradually decreased. As the latent size decreases, SD-VAE tends to collapse, while DGAE still maintains a high fidelity.

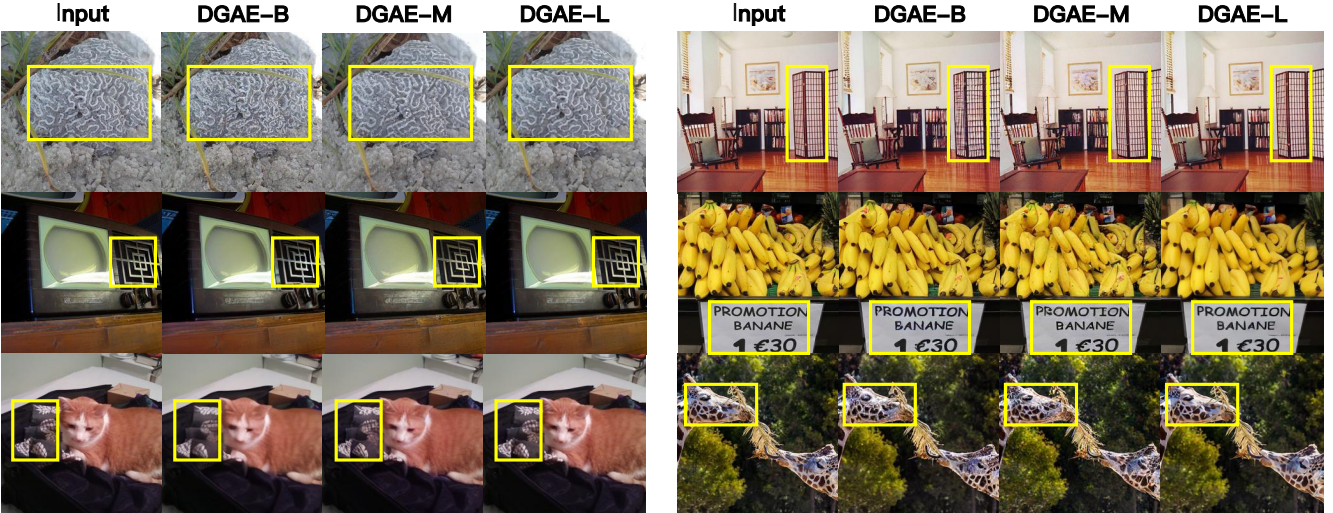


Figure 5: Scalability Evaluation of DGAE. By scaling up the decoder, DGAE achieves better reconstruction quality with enhanced detail preservation.

As shown in table 3, DGAE consistently outperforms SD-VAE across different latent sizes. In particular, even with a latent dimensionality reduced by half, DGAE still achieves superior generation quality, demonstrating the robustness of its latent space. Figure 6

shows samples generated by DiT trained on DGAE’s latent representations with a size of 2048. Even after just 1M training steps, the model is able to produce visually compelling results.

To further understand the benefits of smaller latent sizes, we examined the convergence behavior of DiT models with different latent sizes. As shown in fig. 7, DiT models converge more

**Table 2: DGAE effectively improves the reconstruction performance. As the latent size decreases, the performance of SD-VAE drops significantly, while DGAE remains relatively stable. In addition, during our reproduction of SD-VAE-f32, we found that the GAN was highly prone to collapse, and we did not obtain a reasonable result.**

Spatial downsampling	Latent Shape	Latent Size	Autoencoder	Reconstruction Performance		
				rFID-5k↓	PSNR↑	SSIM↑
f8	$32 \times 32 \times 4$	4096	SD-VAE	4.91	24.60	0.74
			DGAE	4.23	25.73	0.76
f16	$16 \times 16 \times 16$	4096	SD-VAE	4.62	23.90	0.75
			DGAE	3.98	25.33	0.76
f16	$16 \times 16 \times 8$	2048	SD-VAE	8.53	22.62	0.70
			DGAE	4.99	24.46	0.74
f32	$16 \times 16 \times 4$	1024	SD-VAE	16.02	20.97	0.63
			DGAE	9.45	21.54	0.68
f32	$8 \times 8 \times 64$	4096	SD-VAE	9.07	22.26	0.69
			DGAE	5.14	23.07	0.73

**Table 3: Class-conditional generation results on ImageNet 256 × 256 (w/o CFG). With the latent representations learned by DGAE, DiT achieves comparable generation quality using only half the latent dimensionality of SD-VAE. (In specification, 'f' and 'c' represent the spatial downsampling and channel, respectively.)**

Diffusion Model	Autoencoder			Generation Performance			
	Latent Size	Specification	Type	gFID↓	sFID↓	Precision↑	Recall↑
DiT-XL [53]	4096	f16c16	SD-VAE	11.51	5.47	0.67	0.65
			DGAE	10.41	5.39	0.71	0.61
	2048	f16c8	SD-VAE	12.49	5.48	0.68	0.62
			DGAE	11.16	5.43	0.69	0.62

quickly with smaller latent sizes, indicating that diffusion models achieve faster convergence and reduced training costs when utilizing smaller latent dimensions.

Next, we explore why the latent representation learned by DGAE is more effective.

#### 4.4 Latent Representation

The use of KL normalization in SD-VAE involves a trade-off between information capacity and detailed information [76], this requires the decoder to be able to fill in the lost details. Diffusion models, however, possess a unique coarse-to-fine nature: they first synthesize low-frequency signal components and later refine them with high-frequency details. This property appears particularly well-suited for compensating the loss of fine-grained information in the latent space. As shown in fig. 8, we visualized the latent representations of DGAE and SD-VAE separately and found an interesting phenomenon: DGAE has a smoother latent space. This eliminates the burden of learning nonlinear relationships in the latent space for generative models. Based on the smoother latent representation, the decoder is freed up to fill in the details. This may be the reason why DGAE can achieve better reconstruction results with a smaller latent space.



**Figure 6: Class-Conditional Image Generation Results of DiT-XL Trained on ImageNet 256×256. Despite being trained for only 1M steps, DiT-XL achieves high-quality generation on the DGAE’s latent space.**

## 5 Related Work

**Diffusion models.** Diffusion models [30, 37, 39, 48, 51, 53, 70, 77] have supplanted traditional generative models, including GANs [22, 25, 26, 38] and VAEs [15, 28, 40, 62], emerging as the predominant framework in the realm of visual generation. Due to direct optimization in the pixel space and the use of multi-timestep training and

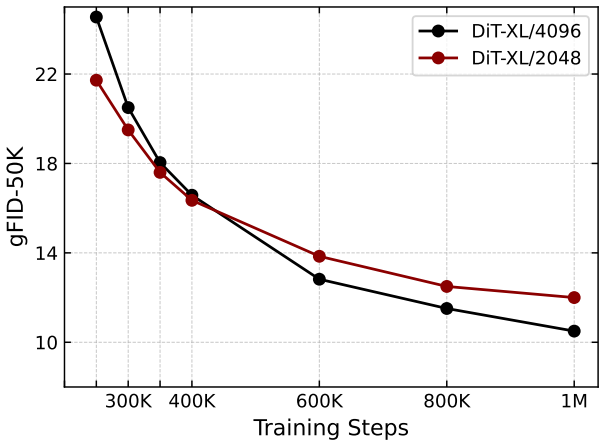


**Figure 7: Convergence Curves of DiT-XL under Different Latent Sizes. As the training steps increases, the DiT-XL trained with a latent size of 2048 converges more quickly.**



**Figure 8: Visualizing the Latent Representations of SD-VAE and DGAE. By applying a simple linear projection to map the latent representations to the RGB space, we observe that DGAE exhibits a smoother latent space compared to SD-VAE, without compromising reconstruction performance.**

inference, diffusion models were initially applied only to the synthesis of low-resolution visual content [30, 37, 51, 77]. To scale them up to high-resolution image generation, subsequent works either adopt super-resolution techniques to increase the generated images to higher resolutions [31, 60, 64] or perform optimization in the latent

space instead of the pixel space [63]. In parallel, another line of research focuses on accelerating the sampling process through methods such as knowledge distillation [65, 66, 68] and noise scheduling [39, 41, 51]. By adopting these strategies, diffusion models have achieved remarkable results in visual generation [3, 4, 6, 8, 9, 11–13, 19, 29, 36, 42, 45, 47, 49, 52, 54–57, 59, 64, 72, 81–86, 90, 93, 94].

**Visual Autoencoders.** Due to the success of LDM’s SD-VAE, substantial efforts have been devoted to developing better autoencoders. To enable a more efficient denoising process, follow-up works have focused on improving reconstruction accuracy under high spatial compression [10, 16, 20, 23, 75].

Another popular trend is employ wavelet transforms to enhance high-frequency details [42, 52, 88]. In addition to the continuous AEs explored in this work, multiple discrete AEs [44, 52, 61, 73, 74, 78, 80, 89, 92] are proposed to aid autoregressive tasks [21, 24, 71].

However, the above methods all incorporate GAN loss as part of their training objective. While this enhances the autoencoder’s ability to capture texture and structural details, it also introduces training instability. Moreover, these approaches primarily focus on improving reconstruction quality, while overlooking the importance of the latent size. To address these limitations, we propose using diffusion models, which provide stable training and better utilize compact latent spaces.

**Diffusion Autoencoders.** Early works incorporate diffusion decoders into autoencoders [1, 58, 67] primarily aimed to leverage the stochastic nature of diffusion processes to enhance image quality, without establishing a clear connection to the latent diffusion modeling (LDM) framework [63]. SWYCC [5] refines the output of an autoencoder by appending a post-hoc diffusion module, while  $\epsilon$ -VAE [91] integrates diffusion decoders directly within the LDM paradigm. Parallel to our work, DiTo [14] introduces a diffusion-based autoencoder for self-supervised learning, with a stronger focus on architectural scalability.

## 6 Conclusion

We demonstrate that the decoder plays a more important role than the encoder in autoencoders. By introducing a diffusion process to assist the decoder in image reconstruction, our DGAE can map images to a smaller latent size without a decrease in precision. Moreover, compared to SD-VAE that employs a GAN, the training process of DGAE is more stable. In addition, we find that diffusion models can converge more quickly at a smaller latent size.

## References

- [1] Roman Bachmann, Jesse Allardice, David Mizrahi, Enrico Fini, Oğuzhan Fatih Kar, Elmira Amirloo, Alaaeldin El-Nouby, Amir Zamir, and Afshin Dehghan. 2025. FlexTok: Resampling Images into 1D Token Sequences of Flexible Length. *arXiv preprint arXiv:2502.13967* (2025).
- [2] Fan Bao, Shen Nie, Kaiwen Xue, Yue Cao, Chongxuan Li, Hang Su, and Jun Zhu. 2023. All are worth words: A vit backbone for diffusion models. In *IEEE/CVF Conf. Comput. Vis. Pattern Recog. (CVPR)*, 22669–22679.
- [3] Fan Bao, Chendong Xiang, Gang Yue, Guande He, Hongzhou Zhu, Kaiwen Zheng, Min Zhao, Shilong Liu, Yaole Wang, and Jun Zhu. 2024. Vidu: a highly consistent, dynamic and skilled text-to-video generator with diffusion models. *CoRR abs/2405.04233* (2024).
- [4] Omer Bar-Tal, Hila Chefer, Omer Tov, Charles Herrmann, Roni Paiss, Shiran Zada, Ariel Ephrat, Junhwa Hur, Yuanzhen Li, Tomer Michaeli, et al. 2024. Lumiere: A space-time diffusion model for video generation. *CoRR abs/2401.12945* (2024).
- [5] Vighnesh Birodkar, Gabriel Barcik, James Lyon, Sergey Ioffe, David Minnen, and Joshua V Dillon. 2024. Sample what you cant compress. *arXiv preprint arXiv:2409.02529* (2024).

[6] Andreas Blattmann, Tim Dockhorn, Sumith Kulal, Daniel Mendelevitch, Maciej Kilian, Dominik Lorenz, Yam Levi, Zion English, Vikram Voleti, Adam Letts, et al. 2023. Stable video diffusion: Scaling latent video diffusion models to large datasets. *CoRR* abs/2311.15127 (2023).

[7] Andreas Blattmann, Robin Rombach, Huan Ling, Tim Dockhorn, Seung Wook Kim, Sanja Fidler, and Karsten Kreis. 2023. Align Your Latents: High-Resolution Video Synthesis with Latent Diffusion Models. In *IEEE/CVF Conf. Comput. Vis. Pattern Recog. (CVPR)*. IEEE, 22563–22575.

[8] Haodong Chen, Lan Wang, Harry Yang, and Ser-Nam Lim. 2024. OmniCreator: Self-Supervised Unified Generation with Universal Editing. *arXiv preprint arXiv:2412.02114* (2024).

[9] Haoxin Chen, Yong Zhang, Xiaodong Cun, Menghan Xia, Xintao Wang, Chao Weng, and Ying Shan. 2024. Videocrafter2: Overcoming data limitations for high-quality video diffusion models. In *IEEE/CVF Conf. Comput. Vis. Pattern Recog. (CVPR)*. 7310–7320.

[10] Junyu Chen, Han Cai, Junsong Chen, Enze Xie, Shang Yang, Haotian Tang, Muyang Li, Yao Lu, and Song Han. 2024. Deep compression autoencoder for efficient high-resolution diffusion models. *arXiv preprint arXiv:2410.10733* (2024).

[11] Junsong Chen, Chongjian Ge, Enze Xie, Yue Wu, Lewei Yao, Xiaozhe Ren, Zhongdao Wang, Ping Luo, Huchuan Lu, and Zhenguo Li. 2024. Pixart-\sigma: Weak-to-strong training of diffusion transformer for 4k text-to-image generation. *CoRR* abs/2403.04692 (2024).

[12] Junsong Chen, Yue Wu, Simian Luo, Enze Xie, Sayak Paul, Ping Luo, Hang Zhao, and Zhenguo Li. 2024. Pixart-\{\delta\}: Fast and controllable image generation with latent consistency models. *CoRR* abs/2401.05252 (2024).

[13] Junsong Chen, Jincheng Yu, Chongjian Ge, Lewei Yao, Enze Xie, Zhongdao Wang, James T. Kwok, Ping Luo, Huchuan Lu, and Zhenguo Li. 2024. PixArt-\alpha: Fast Training of Diffusion Transformer for Photorealistic Text-to-Image Synthesis. In *Int. Conf. Learn. Represent. (ICLR)*.

[14] Yinbo Chen, Rohit Girdhar, Xiaolong Wang, Sai Saketh Ramabhadra, and Ishan Misra. 2025. Diffusion Autoencoders are Scalable Image Tokenizers. *CoRR* abs/2501.18593 (2025). arXiv:2501.18593 doi:10.48550/ARXIV.2501.18593

[15] Bin Dai and David Wipf. 2019. Diagnosing and enhancing VAE models. *arXiv preprint arXiv:1903.05789* (2019).

[16] Xiaoliang Dai, Ji Hou, Chih-Yao Ma, Sam S. Tsai, Jialiang Wang, Rui Wang, Peizhao Zhang, Simon Vandenhende, Xiaofang Wang, Abhimanyu Dubey, Matthew Yu, Abhishek Kadian, Filip Radenovic, Dhruv Mahajan, Kunpeng Li, Yue Zhao, Vladan Petrovic, Mitesh Kumar Singh, Simran Motwani, Yi Wen, Yiwu Song, Roshan Sumbaly, Vignesh Ramanathan, Zijian He, Peter Vajda, and Devi Parikh. 2023. Emu: Enhancing Image Generation Models Using Photogenic Needles in a Haystack. *CoRR* abs/2309.15807 (2023). arXiv:2309.15807 doi:10.48550/ARXIV.2309.15807

[17] Jia Deng, Wei Dong, Richard Socher, Li-Jia Li, Kai Li, and Li Fei-Fei. 2009. ImageNet: A large-scale hierarchical image database. In *2009 IEEE Computer Society Conference on Computer Vision and Pattern Recognition (CVPR 2009), 20-25 June 2009, Miami, Florida, USA*. IEEE Computer Society, 248–255. doi:10.1109/CVPR.2009.5206848

[18] Prafulla Dhariwal and Alexander Nichol. 2021. Diffusion models beat gans on image synthesis. *Advances in neural information processing systems* 34 (2021), 8780–8794.

[19] Runpei Dong, Chunrui Han, Yuang Peng, Zekun Qi, Zheng Ge, Jinrong Yang, Liang Zhao, Jianjian Sun, Hongyu Zhou, Haoran Wei, et al. 2023. Dreamlm: Synergistic multimodal comprehension and creation. *arXiv preprint arXiv:2309.11499* (2023).

[20] Patrick Esser, Sumith Kulal, Andreas Blattmann, Rahim Entezari, Jonas Müller, Harry Saini, Yam Levi, Dominik Lorenz, Axel Sauer, Frederic Boesel, Dustin Podell, Tim Dockhorn, Zion English, and Robin Rombach. 2024. Scaling Rectified Flow Transformers for High-Resolution Image Synthesis. In *Int. Conf. Mach. Learn. (ICML)*.

[21] Patrick Esser, Robin Rombach, and Björn Ommer. 2021. Taming Transformers for High-Resolution Image Synthesis. In *IEEE/CVF Conf. Comput. Vis. Pattern Recog. (CVPR)*. Computer Vision Foundation / IEEE, 12873–12883.

[22] Ian J. Goodfellow, Jean Pouget-Abadie, Mehdi Mirza, Bing Xu, David Warde-Farley, Sherjil Ozair, Aaron C. Courville, and Yoshua Bengio. 2014. Generative Adversarial Nets. In *Adv. Neural Inform. Process. Syst. (NIPS)*. 2672–2680.

[23] Yoav HaCohen, Nisan Chiriput, Benny Brazowski, Daniel Shalem, Dudu Moshe, Eitan Richardson, Eran Levin, Guy Shiran, Nir Zabari, Ori Gordon, et al. 2024. Ltx-video: Realtime video latent diffusion. *arXiv preprint arXiv:2501.00103* (2024).

[24] Jian Han, Jinlai Liu, Yi Jiang, Bin Yan, Yuqi Zhang, Zehuan Yuan, Bingyu Peng, and Xiaobing Liu. 2024. Infinity: Scaling bitwise autoregressive modeling for high-resolution image synthesis. *arXiv preprint arXiv:2412.04431* (2024).

[25] Zhenliang He, Meina Kan, and Shiguang Shan. 2021. Eigengan: Layer-wise eigen-learning for gans. In *Proceedings of the IEEE/CVF international conference on computer vision*. 14408–14417.

[26] Zhenliang He, Wangmeng Zuo, Meina Kan, Shiguang Shan, and Xilin Chen. 2019. AttnGAN: Facial attribute editing by only changing what you want. *IEEE transactions on image processing* 28, 11 (2019), 5464–5478.

[27] Martin Heusel, Hubert Ramsauer, Thomas Unterthiner, Bernhard Nessler, and Sepp Hochreiter. 2017. GANs Trained by a Two Time-Scale Update Rule Converge to a Local Nash Equilibrium. In *Adv. Neural Inform. Process. Syst. (NIPS)*, Isabelle Guyon, Ulrike von Luxburg, Samy Bengio, Hanna M. Wallach, Rob Fergus, S. V. N. Vishwanathan, and Roman Garnett (Eds.). 6626–6637.

[28] Irina Higgins, Loic Matthey, Arka Pal, Christopher Burgess, Xavier Glorot, Matthew Botvinick, Shakir Mohamed, and Alexander Lerchner. 2017. beta-vae: Learning basic visual concepts with a constrained variational framework. In *International conference on learning representations*.

[29] Jonathan Ho, William Chan, Chitwan Saharia, Jay Whang, Ruiqi Gao, Alexey Grigchenko, Diederik P Kingma, Ben Poole, Mohammad Norouzi, David J Fleet, et al. 2022. Imagen video: High definition video generation with diffusion models. *CoRR* abs/2210.02303 (2022).

[30] Jonathan Ho, Ajay Jain, and Pieter Abbeel. 2020. Denoising Diffusion Probabilistic Models. In *Adv. Neural Inform. Process. Syst. (NeurIPS)*.

[31] Jonathan Ho, Chitwan Saharia, William Chan, David J Fleet, Mohammad Norouzi, and Tim Salimans. 2022. Cascaded diffusion models for high fidelity image generation. *Journal of Machine Learning Research* 23, 47 (2022), 1–33.

[32] Alain Hore and Djemel Ziou. 2010. Image quality metrics: PSNR vs. SSIM. In *2010 20th international conference on pattern recognition*. IEEE, 2366–2369.

[33] Aapo Hyvärinen. 2005. Estimation of Non-Normalized Statistical Models by Score Matching. *J. Mach. Learn. Res.* 6 (2005), 695–709.

[34] Phillip Isola, Jun-Yan Zhu, Tinghui Zhou, and Alexei A Efros. 2017. Image-to-image translation with conditional adversarial networks. In *IEEE/CVF Conf. Comput. Vis. Pattern Recog. (CVPR)*. 1125–1134.

[35] Justin Johnson, Alexandre Alahi, and Li Fei-Fei. 2016. Perceptual losses for real-time style transfer and super-resolution. In *Eur. Conf. Comput. Vis. (ECCV)*. Springer, 694–711.

[36] Kumarah Kahatapitiya, Haozhe Liu, Sen He, Ding Liu, Menglin Jia, Chenyang Zhang, Michael S Ryoo, and Tian Xie. 2024. Adaptive caching for faster video generation with diffusion transformers. *arXiv preprint arXiv:2411.02397* (2024).

[37] Tero Karras, Miika Aittala, Timo Aila, and Samuli Laine. 2022. Elucidating the Design Space of Diffusion-Based Generative Models. In *Adv. Neural Inform. Process. Syst. (NIPS)*, Sanmi Koyejo, S. Mohamed, A. Agarwal, Danielle Belgrave, K. Cho, and A. Oh (Eds.). [http://papers.nips.cc/paper\\_files/paper/2022/hash/48846e9d9cc01cfb87eb694d946ce6b-Abstract-Conference.html](http://papers.nips.cc/paper_files/paper/2022/hash/48846e9d9cc01cfb87eb694d946ce6b-Abstract-Conference.html)

[38] Tero Karras, Samuli Laine, and Timo Aila. 2021. A Style-Based Generator Architecture for Generative Adversarial Networks. *IEEE Trans. Pattern Anal. Mach. Intell.* 43, 12 (2021), 4217–4228. doi:10.1109/TPAMI.2020.2970919

[39] Diederik Kingma, Tim Salimans, Ben Poole, and Jonathan Ho. 2021. Variational diffusion models. *Advances in neural information processing systems* 34 (2021), 21696–21707.

[40] Diederik P. Kingma and Max Welling. 2014. Auto-Encoding Variational Bayes. In *Int. Conf. Learn. Represent. (ICLR)*.

[41] Zhipeng Kong and Wei Ping. 2021. On fast sampling of diffusion probabilistic models. *arXiv preprint arXiv:2106.00132* (2021).

[42] PKU-Yuan Lab and Tuzhan AI etc. 2024. *Open-Sora-Plan*. doi:10.5281/zenodo.10948109

[43] Anders Boesen Lindbo Larsen, Søren Kaae Sønderby, Hugo Larochelle, and Ole Winther. 2016. Autoencoding beyond pixels using a learned similarity metric. In *International conference on machine learning*. PMLR, 1558–1566.

[44] Xiang Li, Kai Qiu, Hao Chen, Jason Kuen, Jiuxiang Gu, Bhiksha Raj, and Zhe Lin. 2024. Imagefolder: Autoregressive image generation with folded tokens. *arXiv preprint arXiv:2410.01756* (2024).

[45] Shiyu Liu, Yucheng Han, Peng Xing, Fukun Yin, Rui Wang, Wei Cheng, Jiaqi Liao, Yingming Wang, Honghao Fu, Chunrui Han, et al. 2025. StepIX-edit: A practical framework for general image editing. *arXiv preprint arXiv:2504.17761* (2025).

[46] Siwei Lyu. 2012. Interpretation and Generalization of Score Matching. *CoRR* abs/1205.2629 (2012). arXiv:1205.2629 <http://arxiv.org/abs/1205.2629>

[47] Guoqing Ma, Haoyang Huang, Kun Yan, Liangyu Chen, Nan Duan, Shengming Yin, Changyi Wan, Runchen Ming, Xiaoniu Song, Xing Chen, et al. 2025. Step-video-t2v technical report: The practice, challenges, and future of video foundation model. *arXiv preprint arXiv:2502.10248* (2025).

[48] Nanyi Ma, Mark Goldstein, Michael S Albergo, Nicholas M Boffi, Eric Vandenberghe, and Saining Xie. 2024. SiT: Exploring flow and diffusion-based generative models with scalable interpolant transformers. In *European Conference on Computer Vision*. Springer, 23–40.

[49] Xin Ma, Yaohui Wang, Gengyun Jia, Xinyuan Chen, Ziwei Liu, Yuan-Fang Li, Cunjian Chen, and Yu Qiao. 2024. Latte: Latent diffusion transformer for video generation. *CoRR* abs/2401.03048 (2024).

[50] Charlie Nash, Jacob Menick, Sander Dieleman, and Peter W Battaglia. 2021. Generating images with sparse representations. *arXiv preprint arXiv:2103.03841* (2021).

[51] Alexander Quinn Nichol and Prafulla Dhariwal. 2021. Improved Denoising Diffusion Probabilistic Models. In *Int. Conf. Mach. Learn. (ICML) (Proceedings of Machine Learning Research, Vol. 139)*, Marina Meila and Tong Zhang (Eds.). PMLR, 8162–8171. <http://proceedings.mlr.press/v139/nichol21a.html>

[52] NVIDIA, ;, Niket Agarwal, Arslan Ali, Maciej Bala, Yogesh Balaji, Erik Barker, Tiffany Cai, Prithvijit Chattopadhyay, Yongxin Chen, Yin Cui, Yifan Ding, Daniel Dworakowski, Jiaoqiao Fan, Michele Fenzi, Francesco Ferroni, Sanja Fidler, Dieter Fox, Songwei Ge, Yunhao Ge, Jinwei Gu, Siddharth Gururani, Ethan He, Jiahui Huang, Jacob Huffman, Pooya Jannaty, Jingyi Jin, Seung Wook Kim, Gergely Klár, Grace Lam, Shiyi Lan, Laura Leal-Taixe, Anqi Li, Zhaoshuo Li, Chen-Hsuan Lin, Tsung-Yi Lin, Huan Ling, Ming-Yu Liu, Xian Liu, Alice Luo, Qianli Ma, Hanzi Mao, Kaichun Mo, Arsalan Mousavian, Seungjun Nah, Sriharsha Niverty, David Page, Despoina Paschalidou, Zeeshan Patel, Lindsey Pavao, Morteza Ramezanali, Fitsum Reda, Xiaowei Ren, Vasanth Rao Naik Sabavat, Ed Schmerling, Stella Shi, Bartosz Stefanik, Shitao Tang, Lyne Tchampi, Przemek Tredak, Wei-Cheng Tseng, Jibin Varghese, Hao Wang, Haoxiang Wang, Heng Wang, Ting-Chun Wang, Fangyu Wei, Xinyue Wei, Jay Zhangjie Wu, Jiashu Xu, Wei Yang, Lin Yen-Chen, Xiaohui Zeng, Yu Zeng, Jing Zhang, Qinsheng Zhang, Yuxuan Zhang, Qingqing Zhao, and Artur Zolkowski. 2025. Cosmos World Foundation Model Platform for Physical AI. *CoRR* (2025). arXiv:2501.03575 [cs.CV] <https://arxiv.org/abs/2501.03575>

[53] William Peebles and Saining Xie. 2023. Scalable Diffusion Models with Transformers. In *Int. Conf. Comput. Vis. (ICCV)*. IEEE, 4172–4182.

[54] Xiangyu Peng, Zangwei Zheng, Chenhui Shen, Tom Young, Xinying Guo, Binluo Wang, Hang Xu, Hongxin Liu, Mingyan Jiang, Wenjun Li, et al. 2025. Open-sora 2.0: Training a commercial-level video generation model in \$200 k. *arXiv preprint arXiv:2503.09642* (2025).

[55] Yuang Peng, Yuxin Cui, Haomiao Tang, Zekun Qi, Runpei Dong, Jing Bai, Chunrui Han, Zheng Ge, Xiangyu Zhang, and Shu-Tao Xia. 2025. DreamBench++: A Human-Aligned Benchmark for Personalized Image Generation. In *The Thirteenth International Conference on Learning Representations*, Vol. abs/2406.16855.

[56] Dustin Podell, Zion English, Kyle Lacey, Andreas Blattmann, Tim Dockhorn, Jonas Müller, Joe Penna, and Robin Rombach. 2024. SDXL: Improving Latent Diffusion Models for High-Resolution Image Synthesis. In *Int. Conf. Learn. Represent. (ICLR)*.

[57] Adam Polyak, Amit Zohar, Andrew Brown, Andros Tjandra, Animesh Sinha, Ann Lee, Apoorv Vyas, Bowen Shi, Chih-Yao Ma, Ching-Yao Chuang, et al. 2024. Movie Gen: A Cast of Media Foundation Models. *CoRR* abs/2410.13720 (2024).

[58] Konpat Preechakul, Nattanan Chatthee, Suttisak Wizadwongsu, and Supasorn Suwajanakorn. 2022. Diffusion autoencoders: Toward a meaningful and decodable representation. In *Proceedings of the IEEE/CVF conference on computer vision and pattern recognition*. 10619–10629.

[59] Can Qin, Congying Xia, Krithika Ramakrishnan, Michael Ryoo, Lifu Tu, Yihao Feng, Manli Shu, Honglu Zhou, Anas Awadalla, Jun Wang, et al. 2024. xGen-VideoSyn-1: High-fidelity Text-to-Video Synthesis with Compressed Representations. *CoRR* abs/2408.12590 (2024).

[60] Aditya Ramesh, Prafulla Dhariwal, Alex Nichol, Casey Chu, and Mark Chen. 2022. Hierarchical text-conditional image generation with clip latents. *CoRR* abs/2204.06125 (2022).

[61] Ali Razavi, Aaron Van den Oord, and Oriol Vinyals. 2019. Generating diverse high-fidelity images with vq-vae-2. *Advances in neural information processing systems* 32 (2019).

[62] Danilo Jimenez Rezende and Fabio Viola. 2018. Taming vae’s. *arXiv preprint arXiv:1810.00597* (2018).

[63] Robin Rombach, Andreas Blattmann, Dominik Lorenz, Patrick Esser, and Björn Ommer. 2022. High-Resolution Image Synthesis with Latent Diffusion Models. In *IEEE/CVF Conf. Comput. Vis. Pattern Recog. (CVPR)*. IEEE.

[64] Chitwan Saharia, William Chan, Saurabh Saxena, Lala Li, Jay Whang, Emily L. Denton, Seyed Kamyar Seyed Ghasemipour, Raphael Gontijo Lopes, Burcu Karagol Ayan, Tim Salimans, Jonathan Ho, David J. Fleet, and Mohammad Norouzi. 2022. Photorealistic Text-to-Image Diffusion Models with Deep Language Understanding. In *Adv. Neural Inform. Process. Syst. (NeurIPS)*.

[65] Tim Salimans and Jonathan Ho. 2022. Progressive Distillation for Fast Sampling of Diffusion Models. In *Int. Conf. Learn. Represent. (ICLR)*. OpenReview.net. <https://openreview.net/forum?id=TIdIXIpzhoI>

[66] Axel Sauer, Dominik Lorenz, Andreas Blattmann, and Robin Rombach. 2023. Adversarial diffusion distillation. *CoRR* abs/2311.17042 (2023).

[67] Jie Shi, Chenfei Wu, Jian Liang, Xiang Liu, and Nan Duan. 2022. Divae: Photorealistic images synthesis with denoising diffusion decoder. *arXiv preprint arXiv:2206.00386* (2022).

[68] Yang Song, Prafulla Dhariwal, Mark Chen, and Ilya Sutskever. 2023. Consistency models. (2023).

[69] Yang Song and Stefano Ermon. 2019. Generative Modeling by Estimating Gradients of the Data Distribution. In *Adv. Neural Inform. Process. Syst. (NIPS)*. 11895–11907.

[70] Yang Song, Jascha Sohl-Dickstein, Diederik P. Kingma, Abhishek Kumar, Stefano Ermon, and Ben Poole. 2021. Score-Based Generative Modeling through Stochastic Differential Equations. In *Int. Conf. Learn. Represent. (ICLR)*.

[71] Peize Sun, Yi Jiang, Shoufa Chen, Shilong Zhang, Bingyu Peng, Ping Luo, and Zehuan Yuan. 2024. Autoregressive model beats diffusion: Llama for scalable image generation. *arXiv preprint arXiv:2406.06525* (2024).

[72] Yuqi Tan, Yuang Peng, Hao Fang, Bin Chen, and Shu-Tao Xia. 2024. Waterdiff: Perceptual image watermarks via diffusion model. In *ICASSP 2024-2024 IEEE International Conference on Acoustics, Speech and Signal Processing (ICASSP)*. IEEE, 3250–3254.

[73] Anni Tang, Tianyu He, Junliang Guo, Xinle Cheng, Li Song, and Jiang Bian. 2024. Vidtok: A versatile and open-source video tokenizer. *arXiv preprint arXiv:2412.13061* (2024).

[74] Keyu Tian, Yi Jiang, Zehuan Yuan, Bingyu Peng, and Liwei Wang. 2024. Visual autoregressive modeling: Scalable image generation via next-scale prediction. *Advances in neural information processing systems* 37 (2024), 84839–84865.

[75] Rui Tian, Qi Dai, Jianmin Bao, Kai Qiu, Yifan Yang, Chong Luo, Zuxuan Wu, and Yu-Gang Jiang. 2024. REDUCIO! Generating 1024×1024 Video within 16 Seconds using Extremely Compressed Motion Latents. *arXiv preprint arXiv:2411.13552* (2024).

[76] Michael Tschannen, Cian Eastwood, and Fabian Mentzer. 2023. GIVT: Generative Infinite-Vocabulary Transformers. *ArXiv* abs/2312.02116 (2023). <https://api.semanticscholar.org/CorpusID:265610025>

[77] Arash Vahdat, Karsten Kreis, and Jan Kautz. 2021. Score-based Generative Modeling in Latent Space. In *Adv. Neural Inform. Process. Syst. (NIPS)*, Marc’Aurelio Ranzato, Alina Beygelzimer, Yann N. Dauphin, Percy Liang, and Jennifer Wortman Vaughan (Eds.), 11287–11302. <https://proceedings.neurips.cc/paper/2021/hash/5dca4c6b9e244d24a30b4c45601d9720-Abstract.html>

[78] Aaron Van Den Oord, Oriol Vinyals, et al. 2017. Neural discrete representation learning. *Advances in neural information processing systems* 30 (2017).

[79] Pascal Vincent. 2011. A Connection Between Score Matching and Denoising Autoencoders. *Neural Comput.* 23, 7 (2011), 1661–1674. doi:10.1162/NECO\_A\_00142

[80] Junke Wang, Yi Jiang, Zehuan Yuan, Bingyu Peng, Zuxuan Wu, and Yu-Gang Jiang. 2024. Ommitokenizer: A joint image-video tokenizer for visual generation. *Advances in Neural Information Processing Systems* 37 (2024), 28281–28295.

[81] Shitao Xiao, Yueze Wang, Junjie Zhou, Huaying Yuan, Xingrun Xing, Ruiran Yan, Shuting Wang, Tiejun Huang, and Zheng Liu. 2024. Omnigen: Unified image generation. *CoRR* abs/2409.11340 (2024).

[82] Enze Xie, Junsong Chen, Junyu Chen, Han Cai, Haotian Tang, Yujun Lin, Zhekai Zhang, Muyang Li, Ligeng Zhu, Yao Lu, et al. 2024. Sana: Efficient high-resolution image synthesis with linear diffusion transformers. *arXiv preprint arXiv:2410.10629* (2024).

[83] Yuqiu Xie, Bolin Jiang, Jiawei Li, Naiqi Li, Bin Chen, Tao Dai, Yuang Peng, and Shu-Tao Xia. 2024. GladCoder: stylized QR code generation with grayscale-aware denoising process. In *Proceedings of the Thirty-Third International Joint Conference on Artificial Intelligence*. 7780–7787.

[84] Jinbo Xing, Menghan Xia, Yong Zhang, Hao Chen, Wangbo Yu, Hanyuan Liu, Gongye Liu, Xintao Wang, Ying Shan, and Tien-Tsin Wong. 2024. DynamicalCrafter: Animating Open-Domain Images with Video Diffusion Priors. In *Eur. Conf. Comput. Vis. (ECCV) (Lecture Notes in Computer Science, Vol. 15104)*. Springer, 399–417.

[85] Yifeng Xu, Zhenliang He, Shiguang Shan, and Xilin Chen. 2024. CtrLoRA: An Extensible and Efficient Framework for Controllable Image Generation. *arXiv preprint arXiv:2410.09400* (2024).

[86] Zhouyi Yang, Jiayan Teng, Wendi Zheng, Ming Ding, Shiyu Huang, Jiazheng Xu, Yuanming Yang, Wenyi Hong, Xiaohan Zhang, Guanyu Feng, et al. 2024. Cogvideox: Text-to-video diffusion models with an expert transformer. *CoRR* abs/2408.06072 (2024).

[87] Jingfeng Yao, Bin Yang, and Xinggang Wang. 2025. Reconstruction vs. generation: Taming optimization dilemma in latent diffusion models. *arXiv preprint arXiv:2501.01423* (2025).

[88] Hu Yu, Hao Luo, Hangjie Yuan, Yu Rong, and Feng Zhao. 2025. Frequency Autoregressive Image Generation with Continuous Tokens. *arXiv preprint arXiv:2503.05305* (2025).

[89] Lijun Yu, José Lezama, Nitesh Bharadwaj Gundavarapu, Luca Versari, Kihyuk Sohn, David Minnen, Yong Cheng, Agrim Gupta, Xiuye Gu, Alexander G. Hauptmann, Boqing Gong, Ming-Hsuan Yang, Irfan Essa, David A. Ross, and Lu Jiang. 2024. Language Model Beats Diffusion - Tokenizer is key to visual generation. In *Int. Conf. Learn. Represent. (ICLR)*.

[90] Lvmi Zhang, Anyi Rao, and Maneesh Agrawala. 2023. Adding conditional control to text-to-image diffusion models. In *Proceedings of the IEEE/CVF international conference on computer vision*. 3836–3847.

[91] Long Zhao, Sanghyun Woo, Ziyu Wan, Yandong Li, Han Zhang, Boqing Gong, Hartwig Adam, Xuhui Jia, and Ting Liu. 2024. e-VAE: Denoising as Visual Decoding. *arXiv preprint arXiv:2410.04081* (2024).

[92] Yue Zhao, Yuanjun Xiong, and Philipp Krähenbühl. 2024. Image and video tokenization with binary spherical quantization. *arXiv preprint arXiv:2406.07548* (2024).

[93] Zangwei Zheng, Xiangyu Peng, Tianji Yang, Chenhui Shen, Shenggui Li, Hongxin Liu, Yukun Zhou, Tianyi Li, and Yang You. 2024. Open-Sora: Democratizing Efficient Video Production for All. <https://github.com/hpcatech/Open-Sora>

[94] Deyu Zhou, Quan Sun, Yuang Peng, Kun Yan, Runpei Dong, Duomin Wang, Zheng Ge, Nan Duan, Xiangyu Zhang, Lionel M Ni, et al. 2025. Taming Teacher Forcing

for Masked Autoregressive Video Generation. *arXiv preprint arXiv:2501.12389* (2025).